ARTICLE NO. 78-1133

Numerical Technique for the Triple-Deck Problem

M. Napolitano,* M. J. Werle,† and R. T. Davis‡
University of Cincinnati, Cincinnati, Ohio

An efficient alternating direction implicit numerical technique is developed for solving the triple-deck fundamental problem for supersonic and subsonic flow. Flow past a parabolic hump on a flat plate is considered as a test case. Accuracy and reliability of the method are positively tested vs linearized equation results for a small hump height. Full nonlinear flow patterns are feasible, including mild separation. Numerical difficulties are encountered around the reattachment point for large hump heights.

Nomenclature

A,B,C	= coefficients of the tridiagonal matrix, Eq. (23)
CI	= Cauchy integral
∂,d	= differential signs
D	= total displacement, $D=\delta+hF(x)$
E_i,G_i	= recursion coefficients for Thomas algorithm, Eq. (24)
$F(x)$	= normalized hump profile
h	= hump height parameter
L	= characteristic geometry length
p	= nondimensional pressure
Re	= characteristic Reynolds number, $Re=U_rL/\nu$
t	= nondimensional time
u	= nondimensional longitudinal velocity component
U_r	= reference freestream velocity
v	= nondimensional normal velocity component
x^*	= physical longitudinal coordinate, Fig. 1
x	= lower deck nondimensional longitudinal coordinate
$\bar{x}$	= transposed lower deck longitudinal coordinate
$\tilde{x}$	= shifted x coordinate ($\tilde{x}=x+\Delta x/2$)
y^*	= physical normal coordinate, Fig. 1
y	= lower deck nondimensional normal coordinate
w	= transposed nondimensional normal velocity component
z	= transposed lower deck normal coordinate
δ	= viscous displacement thickness
Δ	= stepsize
ϵ	= triple-deck small perturbation parameter, $\epsilon=Re^{-1/8}$
θ	= Lighthill's constant, $\theta=0.8272\ldots$
λ	= twice the inverse of the time step, $\lambda=2/\Delta t$
ν	= kinematic viscosity
τ_w	= nondimensional wall shear

Subscripts

$1,2,3,i,j,I,J$	= grid point location
x,y,z	= partial derivative (also total for x) with respect to the indicated variable
$-,+$	= location immediately ahead of and behind the indicated one

Superscripts

$(\ )'$	= total derivative
$n,*,n+1$	= time level in the ADI scheme
0	= old time level value

Introduction

IN recent years, the problem of high Reynolds number laminar separation has received a systematic analysis through the asymptotic triple-deck theory of Stewartson and co-workers,[1-3] Sychev,[4] Neiland,[5,6] and Messiter.[7] Stewartson,[3] in particular, has shown that in many cases of practical interest, for sufficiently small separation-causing disturbances, the structure of the separation region can be represented analytically by a three-layer model which he named the "triple-deck." Three regions are identified—the inner, middle and outer decks—all having characterstic longitudinal length of order ϵ^3L and normal height of order ϵ^5L, ϵ^4L, and ϵ^3L, respectively (Fig. 1). L is the characteristic length of the geometry and ϵ is the small parameter in the perturbation expansion related to the large characteristic flow Reynolds number by the relation $\epsilon^8=1/Re$. These three regions or decks are characterized by viscous, inviscid-rotational, and potential flow conditions, respectively, and their structure and properties are described to first order in the perturbation parameter ϵ by the fundamental triple-deck problem. This consists of the bottom deck, boundary-layer-like equations coupled to a pressure interaction law relating the viscous displacement thickness growth and the inviscid outer deck pressure gradient, according to linear airfoil theory.

Solutions to the triple-deck equations are important for two reasons: first, they provide rational, complete solutions for high Reynolds number flows where the classical boundary-layer approach fails (e.g., in regions where separation and reattachment occur); second, they offer a reliable test base for assessing more comprehensive flow equation solvers (e.g., numerical algorithms for the Navier-Stokes or interacting boundary-layer equations[10]). To date, only a limited number of such solutions have been obtained for this general equation set. Solutions are available, for example, for the free interaction phenomenon between a shock wave and a boundary-layer flow,[2,12] for supersonic flow past compression and expansion corners,[13-15] and forward and backward facing steps.[15] Subsonic flow at the trailing edge of a finite flat plate has also been studied by several investigators independently.[7,16,17] Finally, it has been postulated[4,18] and later

Received July 5, 1978, presented as Paper 78-1133 at the AIAA 11th Fluid and Plasma Dynamics Conference, Seattle, Wash., July 10-12, 1978; revision received Feb. 2, 1979.

Index categories: Computational Methods; Subsonic Flow; Supersonic and Hypersonic Flow.

*Research Associate Aerospace Engineering and Applied Mechanics Dept.; presently, Assistant Professor, University of Bari, Italy. Member AIAA.

†Professor Aerospace Engineering and Applied Mechanics Dept.; presently, Chief, Gas Dynamics Section, United Technology Research Center, East Hartford, Conn. Member AIAA.

‡Professor Aerospace Engineering and Applied Mechanics Dept. Associate Fellow AIAA.

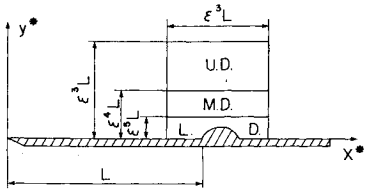

Fig. 1 Triple-deck structure around a small hump.

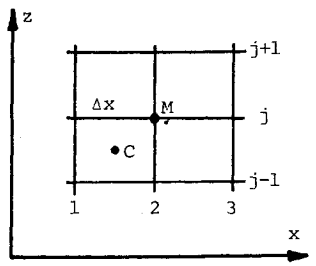

Fig. 2 Computational grid.

numerically proved[19] that this set of equations correctly describes the structure of catastrophic separation as in the flow past a circular cylinder.

While definite advances are being made in the understanding of interacting flows through use of the triple-deck concept, progress is being slowed by the general inefficiency of most solution techniques available for this problem in the literature. These, due to the boundary value and highly nonlinear nature of the problem, are usually iterative procedures with two or more nested iteration loops which require a large amount of computational effort.[16] For the subsonic case, in particular, numerical convergence is extremely slow and delicate: severe underrelaxation is required and, in some cases, an initialization reasonably close to the sought-after solution is necessary to avoid divergent behavior.

In the present study, the alternating direction implicit (ADI) approach, developed by Werle and Vatsa[20] for solving the supersonic interacting boundary-layer equations, is generalized to provide an efficient triple-deck solver for both supersonic and subsonic flow. Results are presented for supersonic as well as subsonic flow past the parabolic hump of Figs. 1 (physical scaling) and 3 (bottom deck scaling), linearized solutions for a small hump height h being available in the literature.[8] Wall shear and pressure distribution profiles are presented for a wide range of flow conditions including separation.

Governing Equations

For high Reynolds number flow past a hump, $hF(x)=[hx(1-\theta x)]/\theta$, on a flat plate (Figs. 1 and 3). The triple-deck equations are given by Smith[8] as

$$u_x+v_y=0 \tag{1a}$$

$$uu_x+vu_y=-\mathrm{d}p/\mathrm{d}x+u_{yy} \tag{1b}$$

with boundary conditions

$$u[x,hF(x)]=v[x,hF(x)]=0 \tag{2}$$

and

$$u(x,y\to\infty)\to y-\delta-hF(x) \tag{3}$$

In Eq. (1b) the pressure gradient is not a prescribed function as in the classical boundary-layer theory, but is determined through interaction with the displacement thickness δ according to linear airfoil theory. Such an interaction law for supersonic flow conditions is given as

$$\frac{\mathrm{d}^2}{\mathrm{d}x^2}(\delta+hF)=\frac{\mathrm{d}p}{\mathrm{d}x} \tag{4}$$

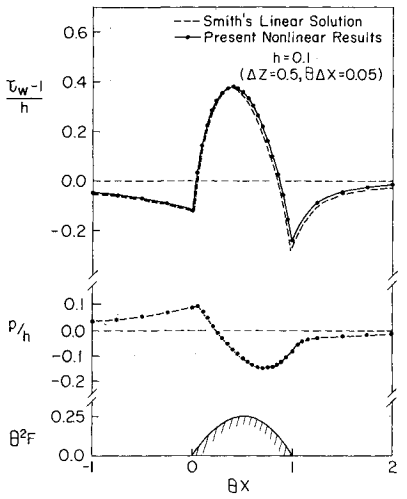

Fig. 3 Hump geometry and supersonic flow, normalized wall shear and pressure profiles.

whereas, in the case of subsonic flow, it is given as

$$\frac{\mathrm{d}^2}{\mathrm{d}x^2}(\delta+hF)=\frac{1}{\pi}\oint_{-\infty}^{\infty}\frac{p_\xi}{x-\xi}\mathrm{d}\xi \tag{5}$$

where the integral is a Cauchy principal value one. Far ahead of the disturbing hump, the flow is a well-developed Blasius boundary layer, which, in the bottom deck scaling, is a uniform shear flow. That is,

$$u(x\to-\infty,y)\to y \tag{6}$$

Also, far ahead of and behind the hump, the disturbance δ dies out and

$$\delta(x\to-\infty)\to 0 \tag{7a}$$

$$\delta(x\to+\infty)\to 0 \tag{7b}$$

The Prandtl transposition theorem[21] can be applied to Eqs. (1-6) in order to make the longitudinal axis coincide with the body surface. This was accomplished here, as in previous supersonic triple-deck solutions,[13-15] by defining new longitudinal and vertical independent variables and a new normal velocity component as

$$\tilde{x}=x \tag{8a}$$

$$z=y-hF(x) \tag{8b}$$

$$w=v-uhF'(x) \tag{8c}$$

By chain-rule differentiation, Eqs. (1) are seen to be invariant under transformations, Eqs. (8), with the advantage that Eqs. (2) become

$$u(\tilde{x},0)=w(\tilde{x},0)=0 \tag{9}$$

which are suitable for use in a constant grid, finite-difference, numerical procedure.

For configurations where the body surface $hF(x)$ has discontinuous slope at one or more points (x) along the surface, the use of the Prandtl transposition theorem introduces a discontinuity in w which, for the supersonic flow case, can be accommodated by the following "jump" condition[15,24]:

$$w(x_+)=w(x_-)+u(x)h[F'(x_-)-F'(x_+)] \tag{10}$$

Numerical Method

ADI Relaxation Technique

The numerical procedure developed here for solving the fundamental triple-deck problem given in Eqs. (1-7) is very

similar to the one successfully applied by Werle and Vatsa[20] to the solution of the supersonic interacting boundary-layer equations in Levy-Lees variables. A relaxation-type time derivative for the total displacement $D(D=\delta+hF)$ is added to the right-hand side of the momentum equation to give§:

$$uu_x + wu_z = -p_x + u_{zz} + \frac{\partial D}{\partial t} \tag{11}$$

and a two-sweep relaxation technique proceeds in time from the nth step to the $(n+1)$th step in two increments of $\Delta t/2$. Over the first half time step (called the * step), Eq. (11) is written as

$$(uu_x + wu_z - u_{zz})^* = -p_x^n + \frac{2}{\Delta t}(D^* - D^n) \tag{12a}$$

whereas, over the second half time step to time t^{n+1}, it becomes

$$(uu_x + wu_z - u_{zz})^* = -p_x^{n+1} + \frac{2}{\Delta t}(D^{n+1} - D^*) \tag{12b}$$

to give a formally second-order accurate solution in Δt. Equation (12a), together with continuity Eq. (1a), constitutes a set of parabolic partial-differential equations which is solved by a marching technique to provide the values of u^*, w^*, D^*.

The second sweep, Eq. (12b), is first simplified using Eq. (12a) to give

$$p_x^{n+1} = p_x^n + \lambda(D^{n+1} - 2D^* + D^n) \tag{13}$$

where $\lambda = 2/\Delta t$ has been introduced for convenience. This, with the use of the interaction laws, Eqs. (4) and (5), becomes

$$D_{xx}^{n+1} = D_{xx}^n + \lambda(D^{n+1} - 2D^* + D^n) \tag{14}$$

and

$$D_{xx}^{n+1} = \oint \frac{p_\xi^n + \lambda(D^{n+1} - 2D^* + D^n)}{x - \xi}\, d\xi \tag{15}$$

for supersonic and subsonic flow, respectively.

Note that Eqs. (14) and (15) carry the boundary value nature of the problem and allow for direct use of a downstream boundary condition for D^{n+1}.

First Sweep Finite-Difference Equations and Superposition Technique

Figure 2 shows the computational grid used in the present numerical scheme. The finite-difference continuity and momentum equations are centered at points C and M, respectively, and are given as follows:

Continuity:

$$\frac{u_{2,j}^* - u_{1,j}^*}{\Delta x} + \frac{u_{2,j-1}^* - u_{1,j-1}^*}{\Delta x} + \frac{w_{2,j}^* - w_{2,j-1}^*}{\Delta z} + \frac{w_{1,j}^* - w_{1,j-1}^*}{\Delta z} = 0 \tag{16}$$

Momentum:

$$\frac{u_{1,j}^* + |u_{1,j}^*|}{2}\frac{u_{2,j}^* - u_{1,j}^*}{\Delta x} + \frac{u_{1,j}^* - |u_{1,j}^*|}{2}\frac{u_{3,j}^0 - u_{2,j}^*}{\Delta x} + \frac{1}{2}w_{1,j}^*\frac{u_{2,j+1}^* - u_{2,j-1}^*}{2\Delta z} + \frac{1}{2}w_{2,j}^*\frac{u_{1,j+1}^* - u_{1,j-1}^*}{2\Delta z} + (p_x^n)_2$$

$$-\lambda(D_2^* - D_2^n) - \frac{u_{2,j+1}^* - 2u_{2,j}^* + u_{2,j-1}^*}{\Delta z^2} = 0 \tag{17}$$

Note that the two convective terms in Eq. (17) have been linearized or quasilinearized around the previous station, 1. Also, note that a windward differencing has been used for the longitudinal convective term uu_x in order to maintain stability of the algorithm in regions of reverse flow. For this case $(u_{1,j}^* < 0)$ the $u_{3,j}^*$ value was taken at the old * time level, $u_{3,j}^0$. Equations (16) and (17) are both linear in their unknowns $u_{2,j}^*$ and $w_{2,j}^*$, which linearly depend on the unknown total displacement D_2^*. A simple superposition technique can then be used to solve the set without iteration. Two new dependent variables, which replace each of the original ones, are defined as:

$$u_{2,j}^* = U_j + D_2^* \tilde{u}_j \tag{18a}$$

$$w_{2,j}^* = W_j + D_2^* \tilde{w}_j \tag{18b}$$

and are then introduced into Eqs. (16) and (17). The resulting two sets of linear finite-difference equations for U_j, W_j and $\tilde{u}_j$, $\tilde{w}_j$ are straightforwardly inverted using the Davis coupled scheme.[22] The total displacement D_2^* is then evaluated by means of the outer boundary condition, Eq. (3), as

$$D_2^* = (z_J - U_J + hF_2)/(1 + \tilde{u}_J) \tag{19}$$

where J indicates the outer edge grid location, and the total velocity components $u_{2,j}^*$, $w_{2,j}^*$ are finally obtained by means of Eqs. (18). (Reference 24 gives the details of the numerical scheme, together with an alternate procedure for evaluating D_2^*.)

In order to properly account for a discontinuous w at the two locations $(x=0$ and $x=1/\theta)$ where $F'(x)$ is discontinuous, a grid point was always chosen to coincide with either location. After obtaining the value $w^*(x_-)$ by means of Eqs. (16) and (17), it was replaced by $w^*(x_+)$ as given in Eq. (10) in order to proceed to the next station $x+\Delta x$. For the subsonic flow case (in the absence of a known jump condition for w), the following finite-difference representations were used for the continuity equation and for the convective term wu_z in the momentum equation.

$$u_x + w_z = \frac{1}{2}\frac{u_{2,j}^* - u_{1,j}^*}{\Delta x} + \frac{1}{2}\frac{u_{2,j-1}^* - u_{1,j-1}^*}{\Delta x} + \frac{w_{2,j}^* - w_{2,j-1}^*}{\Delta z} = 0 \tag{20}$$

$$wu_z = w_2^*\frac{u_{1,j+1}^* - u_{1,j-1}^*}{2\Delta z} \tag{21}$$

The foregoing finite-difference representations eliminate the presence of the unknown w_1 array and avoid differencing across the jump point. They are, therefore, perfectly legitimate as long as $u_{2+} = u_{2-}$, that is, if the u velocity component is continuous across the jump, which it is.

Second Sweep Finite-Difference Equations—Supersonic Flow

The finite-difference form of the supersonic flow second sweep equation is obtained from Eq. (14) by using central differences to approximate the second derivative for the total displacement D_{xx} (which is continuous everywhere). The resulting tridiagonal set of linear algebraic equations is given as:

$$\frac{1}{\Delta x^2}D_{i-1}^{n+1} - \left(\frac{2}{\Delta x^2} + \lambda\right)D_i^{n+1} + \frac{1}{\Delta x^2}D_{i+1}^{n+1} = \frac{D_{i-1}^n - 2D_i^n + D_{i+1}^n}{\Delta x^2} + \lambda(D_i^n - 2D_i^*) \tag{22}$$

§Note that Eq. (11) is not the unsteady bottom deck momentum equation which would contain the longitudinal velocity time derivative, $\partial u/\partial t$, and therefore only the "relaxed" solution will have physical meaning. Also for convenience, the ~ above the x is omitted from Eq. (11) onward.

Even though the direct inversion of Eq. (22) by the Thomas algorithm[26] is a standard technique, it is briefly outlined here to provide a more complete numerical treatment of the downstream boundary condition. Equation (22) is of the form

$$A\,D_{i-1}^{n+1} + B\,D_i^{n+1} + C\,D_{i+1}^{n+1} = H_i \tag{23}$$

and can be directly inverted by the simple recursion formula

$$D_i^{n+1} = E_i D_{i-1}^{n+1} + G_i \tag{24}$$

where the coefficients E_i and G_i are given, respectively, as

$$E_i = \frac{-A}{B + CE_{i+1}} \tag{25a}$$

$$G_i = \frac{H_i - CG_{i+1}}{B + CE_{i+1}} \tag{25b}$$

It can be shown[24] that the most consistent representation of the asymptotic downstream boundary condition is given by

$$E_1 = 1 + \frac{\lambda\Delta x^2}{2} - \sqrt{\left(1 + \frac{\lambda\Delta x^2}{2}\right)^2 - 1} \tag{26a}$$

and

$$G_1 = \frac{2}{\lambda}\left\{-\frac{\lambda\Delta x^2}{2} H_1\right\} \Big/ \left[\frac{\lambda\Delta x^2}{2} + \sqrt{\left(1 + \frac{\lambda\Delta x^2}{2}\right)^2 - 1}\right\} \tag{26b}$$

respectively. (Subscript 1 indicates the downstream boundary condition grid point.)

Subsonic Flow

In order to solve the subsonic flow second sweep equation (15) numerically, the second derivative D_{xx}^{n+1} is first replaced by a central finite-difference representation and the Cauchy integral on the right-hand side is broken into two parts to give

$$\frac{D_{i+1}^{n+1} - 2D_i^{n+1} + D_{i-1}^{n+1}}{\Delta x^2} = \oint_{-\infty}^{\infty} \frac{1}{\pi} \frac{p_\xi^n \mathrm{d}\xi}{x - \xi}$$

$$+ \frac{\lambda}{\pi} \oint_{x_1}^{x_1} \frac{D^{n+1} - 2D^* + D^n}{x - \xi} \mathrm{d}\xi \tag{27}$$

Note that $p_\xi^n(\xi)$ is a known function at all the grid points inside the numerical integration region $x_1 - x_1$. The leading contributor to

$$\oint_{-\infty}^{\infty} \frac{p_\xi^n \mathrm{d}\xi}{x - \xi} \text{ is } \oint_{x_1}^{x_1} \frac{p_\xi^n \mathrm{d}\xi}{x - \xi}$$

and can be evaluated numerically by the method described in Ref. 24; whereas, the residuals

$$\int_{-\infty}^{x_1} \frac{p_\xi^n \mathrm{d}\xi}{x - \xi} \text{ and } \int_{x_1}^{\infty} \frac{p_\xi^n \mathrm{d}\xi}{x - \xi}$$

can be assessed if the asymptotic decay of $p(x)$ is known far ahead of and far behind the region of disturbance (see Ref. 24 for details). It was found here that they did not contribute significantly to the total integral. Also note that in Eq. (27) the Cauchy integral of the relaxation time-dependent term has been approximated with its value over the region of numerical integration only, since its purpose is to allow the solution to relax to its steady-state value and, after this has been reached, the integral vanishes.

Since a full matrix must be inverted to solve Eq. (27) (due to the presence of D_i^{n+1} in the Cauchy integral), the following iterative procedure has been used in order to repeatedly use the very fast Thomas inversion algorithm. The upper and lower diagonal entries for the D_i^{n+1} array are extracted from the Cauchy integral and all the others are replaced with their previous iteration values to give

$$\left(\frac{1}{\Delta x^2} + \frac{\lambda}{\pi}\ell n 3\right) D_{i-1}^{n+1} - \frac{2}{\Delta x^2} D_i^{n+1} + \left(\frac{1}{\Delta x^2} - \frac{\lambda}{\pi}\ell n 3\right) D_{i+1}^{n+1} = H_i \tag{28}$$

In Eq. (28), the $\lambda\ell n 3/\pi$ coefficients come from the corresponding D^{n+1} terms in the Cauchy integral and H_i accounts for all the remaining known right-hand side of Eq. (27) (see Ref. 24 for details). The inversion procedure for Eq. (28), identical now to the one used for the second sweep equation in the supersonic case, must be repeated until some convergence criterion for D_i^{n+1} is met at every location, x_i. As in many previous studies,[16,17] under-relaxation was found necessary to avoid divergent behavior. At the end of each iteration the new value of D_i^{n+1}, obtained by inverting the tridiagonal matrix, was under-relaxed with a factor of 0.2. Other under-relaxation coefficients were found to provide convergent behavior for the second sweep equation, but no systematic numerical study was made in order to find the optimal value. It was found that the relaxation parameter had to be lower than 0.5 in order to obtain convergent behavior. The asymptotic downstream boundary conditions for Eq. (28) are shown[24] to be:

$$E_1 = \left(1 - \frac{\lambda\ell n 3}{\pi}\Delta x^2\right) \Big/ \left(1 + \frac{\lambda\ell n 3}{\pi}\Delta x^2\right) \tag{29a}$$

and

$$G_1 = \frac{H_1 \Delta x^2}{E_1\left(1 + \dfrac{\ell n 3}{\pi}\Delta x^2 - 2\right)} \tag{29b}$$

G_1 was found to become practically zero in all converged numerical computations, but in some computations it grew without bound, thus inducing divergent behavior in the numerical procedure. Setting G_1 identically equal to zero (which it is to second-order accuracy in Δx) was sufficient to remove this problem without deteriorating the accuracy of the solution. A discontinuity occurs in the pressure gradient at the corner points[8] which needs special attention in the $n+1$ time step[1] Cauchy integral evaluation. A satisfactory treatment of this problem is described in Ref. 24. Here, an alternate approach (also used in Ref. 24 for providing a further check of the results) will be described in detail.

Alternate Approach for Subsonic Flow

Most numerical schemes for solving the subsonic triple-deck equations[16,17] use the following interaction law expression

$$D_x = \frac{1}{\pi} \oint_{-\infty}^{\infty} \frac{p(\xi)\,\mathrm{d}\xi}{x - \xi} \tag{30}$$

This can be obtained easily from Eq. (5) by simple integration by parts, which gives

$$\frac{\mathrm{d}D_x}{\mathrm{d}x} = \frac{1}{\pi}\left[\frac{p(\xi)}{x - \xi}\right]_{-\infty}^{\infty} + \frac{\mathrm{d}}{\mathrm{d}x}\frac{1}{\pi}\oint_{-\infty}^{\infty} \frac{p(\xi)\,\mathrm{d}\xi}{x - \xi} \tag{31}$$

At any finite value of x, the first term in the right-hand side of Eq. (31) is seen to identically vanish and Eq. (31) can be straightforwardly integrated to produce Eq. (30). In order to

use Eq. (3) in the second sweep of the present scheme, this is first written in finite-difference form as:

$$\frac{D_i^{n+1}-D_{i-1}^{n+1}}{\Delta x}=\frac{1}{\pi}\oint_{x_I}^{x_I}\frac{p\,d\xi}{x-\xi}=CI(\bar{x}_i) \tag{32}$$

In Eq. (32) the finite-difference representation for D_x^{n+1} is centered at the midpoint $\bar{x}_i$ ($\bar{x}_i=x_i+\Delta x/2$) to avoid any differencing across the jump point, and the numerical evaluation of the Cauchy integral $CI(\bar{x}_i)$ presents no difficultly, since $p(\xi)$ is piecewise continous throughout. Also, note that $CI(\bar{x}_i)$ can be evaluated at every location $\bar{x}_i$ once for every second sweep and used in all the inner loop iterations, since $p(\xi)$ is a known function obtained from dp/dx by numerical quadrature. Equation (32) is then differenced once to give

$$\left(\frac{D_{i+1}^{n+1}-D_i^{n+1}}{\Delta x}-\frac{D_i^{n+1}-D_{i-1}^{n+1}}{\Delta x}\right)\Big/\Delta x=\frac{CI(\bar{x}_{i+1})-CI(\bar{x}_i)}{\Delta x} \tag{33}$$

which is conservative in nature and, therefore, exactly reproduces by integration the perfectly legitimate Eq. (32). Finally, the relaxation integral

$$\oint_{x_I}^{x_I}\frac{\lambda}{\pi}\frac{D^{n+1}-2D^*+D^n}{x-\xi}d\xi$$

is added to the right-hand side of Eq. (33) to formally give

$$\frac{D_{i+1}^{n+1}-2D_i^{n+1}+D_{i-1}^{n+1}}{\Delta x^2}=\frac{CI(\bar{x}_{i+1})-CI(\bar{x}_i)}{\Delta x}$$

$$+\frac{\lambda}{\pi}\oint_{x_I}^{x_I}\frac{D^{n+1}-2D^*+D^n}{x-\xi}d\xi \tag{34}$$

which can be reduced to tridiagonal form exactly as Eq. (27) and inverted by the Thomas algorithm. The advantage with respect to Eq. (27) is in the evaluation of the Cauchy integral for the pressure, which has now removed the singular behavior at the jump point, due to the local pressure gradient discontinuity.

It was found that the length of the region of integration for the Cauchy integral for pressure was extremely critical to the convergence property of this method and, if the integration was limited to the region x_I-x_I as in the previous case, divergent behavior invariably was observed. A study of this point indicated that neglecting the residual of the Cauchy integrals far aft of the disturbance was the source of difficulty. It was found that simply adding $p(x_I)\ell n(x_I-\bar{x}_i)/\pi$ to the value of $CI(\bar{x}_i)$ given in Eq. (32) eliminated the problem and produced a convergent behavior. We believe that improper accounting of this "source-like" term is the main cause of the convergence difficulties faced by many schemes using the interaction law, Eq. (30) (see, for example, Ref. 17).

Results

Supersonic Flow

The present algorithm was applied to the problem of flow past Smith's[8] parabolic hump $[hx(1-\theta x)]/\theta$ of Figs. 1 and 3. A small hump height ($h=0.1$) was first taken into consideration in order to check the present scheme by direct comparison with Smith's linear results.[8] Figure 3 provides a comparison between the normalized wall shear and pressure obtained by the present numerical scheme for the nonlinear set of equations and Smith's linear solutions.[8] The agreement is quite convincing and no other comparisons were sought. Moreover, the numerical scheme was verified to be first-order accurate in the x direction and second-order accurate in the z direction by stepsize studies presented in Ref. 24. Attention was then devoted to higher values of h to assess the influence of nonlinearities, in particular, to predict the onset of separation. Figure 4 presents the normalized pressure profiles for h as high as 4 and Fig. 5 the wall shear (obtained as a three-point, second-order accurate representation for $\partial u/\partial z$) for h as high as 6. Linear theory is seen to provide a fair estimate of the pressure distribution for $h\leq 2$ (Fig. 4), and also to correctly predict the location of separation (Fig. 5) which does, indeed, first occur around the trailing edge of the hump. Figure 5 also confirms the capability of the present scheme of properly assessing mildly separated flowfields.

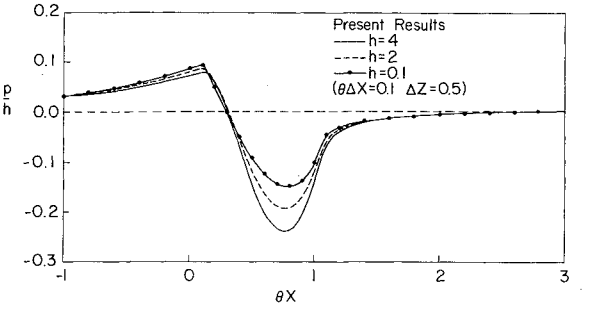

Fig. 4 Supersonic flow, normalized pressure dependence on h.

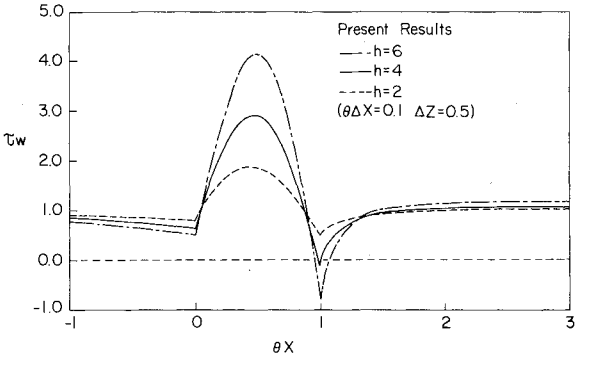

Fig. 5 Subsonic flow, wall shear dependence on h.

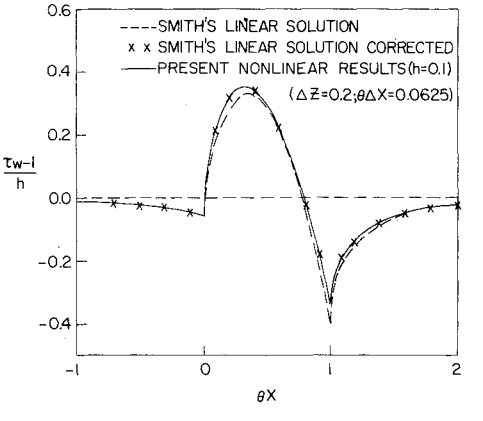

Fig. 6 Subsonic flow, normalized wall shear profile for $h=0.1$.

In the present study, the outer edge boundary conditions were imposed at $z=10$ for the smaller h values and $z=15$ for the higher ones. In all cases it was numerically verified that the u velocity profile became linear ($u\to z-\delta$) over several meshes below the outer edge. The upstream initial and downstream boundary conditions were set at $x=-5$ and $x=15$, respectively, and were numerically verified to be at a sufficient distance, since further increase of the region of integration produced no appreciable change in the results. The numerical procedure was found to converge (average absolute error on the total displacement height ($[\Sigma|D_i^{n+1}-D_i^n|]/(I-$

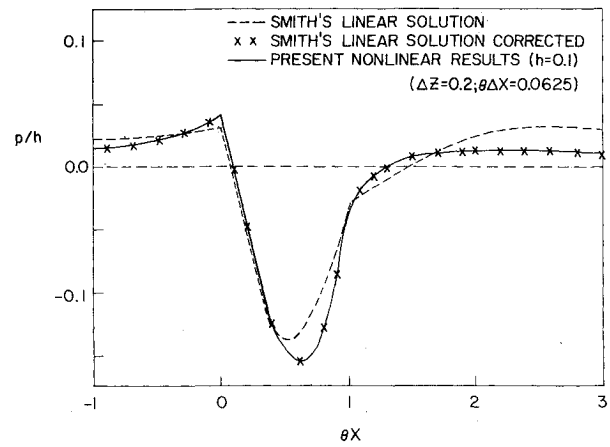

Fig. 7 Subsonic flow, normalized pressure profile for $h = 0.1$.

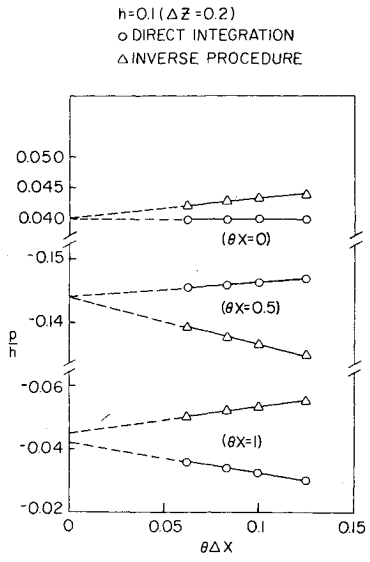

Fig. 8 Subsonic flow, longitudinal stepsize study for pressure.

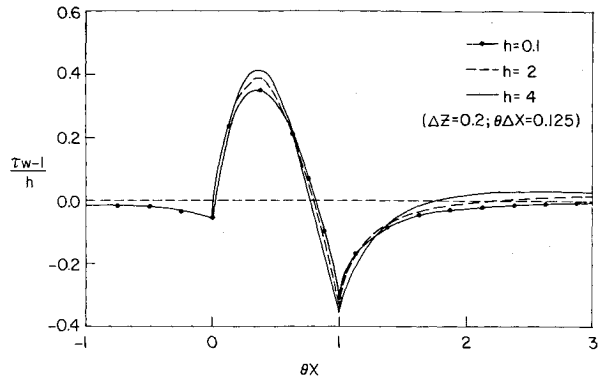

Fig. 9 Subsonic flow, normalized wall shear dependence on h.

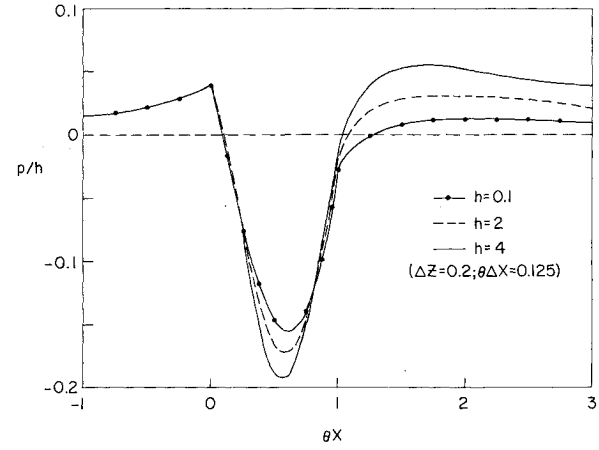

Fig. 10 Subsonic flow, normalized pressure dependence on h.

$1) < 10^{-6}$) within 20 iterations (for h up to 1) and the computer time required for a typical case ($\theta\Delta x = 0.1$, $\Delta z = 0.25$, corresponding to 201 by 41 element matrices for the u and w velocities) was about 15 CPU seconds (AMDAHL 470, double-precision arithmetic). The approximate optimal time step for convergence was numerically found to be given by $\lambda = 1$. In the presence of separation, convergence became slower and λ had to be increased up to 6 (for $h = 6$) to avoid divergent behavior. For the present geometry it is felt that $h = 6$ is close to the highest values of h for which the present scheme could converge because of the large gradients due to the geometry itself. The same scheme and a totally second-order-accurate version of the same were also found to be very efficient for supersonic flow past a wedge. In this case, convergence was easily obtained for normalized wedge angles up to three, corresponding to a fairly large separation bubble, and the results agreed very well with those given in the literature.[13-15]

At the initial time level the pressure gradient and displacement thickness were taken equal to zero at all x_i locations in order to start the relaxation procedure. This physically corresponds to the introduction of the disturbing hump at time equal zero in an otherwise undisturbed uniform shear flow. For the higher hump height cases, h was increased in gradual steps at every new time level t^n until the final value was reached. This was done to avoid the divergent behavior produced by an otherwise too large time rate of change in the transient solution, which, as already mentioned, has no physical meaning anyway.

Subsonic Flow

The subsonic version of the present scheme was applied to flow past the same hump, for which linearized equation results are provided again by Smith.[8] (A quartic hump having continuous slope throughout, for which a numerical solution corresponding to a fairly large separation bubble is given by Sykes,[23] was also considered.[24])

The small hump height $h = 0.1$ was again considered as a test case in order to compare the present numerical results with Smith's linear ones.[8] Figures 6 and 7 show such a comparison for normalized wall shear and pressure profiles. Whereas a reasonable agreement is obtained for the case of the shear, the two pressure distributions show disturbing differences especially immediately upstream and downstream of the hump. Smith has kindly recalculated the pressure and shear profiles and his "corrected" results are now indistinguishable from the present ones.[25]

A longitudinal stepsize study has been performed in order to assess the accuracy and reliability of the solution technique. Wall shear and pressure both resulted in first-order accuracy vs Δx.[24] Here, only the results for pressure are shown in Fig. 8 for three different locations ($\theta x = 0$, 0.5, 1). Two different pressure results are shown for each location x. The circles indicate the pressure values obtained by simple Euler quadrature of the pressure gradient distribution at the final time step $n+1$, after convergence has been reached. The squares indicate the values obtained by a second approach, exploiting the reciprocity property of the Riemann integrals. In fact, besides the interaction law, Eq. (30), the following conjugate integral expression is also true,

$$p = -\frac{1}{\pi} \oint_{-\infty}^{\infty} \frac{D_\xi}{x - \xi} \, d\xi \tag{35}$$

Therefore, after the converged solution has been reached by means of the present numerical scheme, the pressure was evaluated using Eq. (35) and the methods of Ref. 24. The two different pressure evaluations are shown in Fig. 8 to be both first-order accurate, and at locations $\theta x = 0$ as well as $\theta x = 0.5$ they tend to the same limit values as Δx goes to zero. For $\theta x = 1$, the extrapolated results are slightly different, probably because a finite-integration region was used for the Cauchy integrals.

The effect of the finite Δz step was also investigated, but it was found to be negligible at the level of $\Delta z = 0.2$ used in all present calculations.

Just as in the case of supersonic flow, the height of the hump was increased to order one levels in order to investigate the possibility of separation. Figures 9 and 10, respectively, present normalized wall shear and pressure distributions for values of h as high as 4. The $h = 4$ shear profile indicates a region of negative values indicating that, as in the case of supersonic flow, subsonic flow separation also occurs first at the rear end of the hump.[8]

The outer edge boundary conditions were imposed at $z = 8$-15 with increasing h. The range of integration in the longitudinal direction was taken to be $-5 \le \theta x \le 8$ and moving the range further upstream and downstream of the two limits was seen to produce minor changes in the solution. Also, introducing the downstream far-field asymptotic evaluation of the Cauchy integral residual as described in Ref. 14 was seen to modify the results by about 2% or less. Optimizing the procedure could probably have produced the same level of accuracy with a shorter numerical integration region, but this aspect was not pursued further at the present time. All the results presented here have the Cauchy integral region of integration limited to the range $-5 \le \theta x \le 8$.

The approximate optimal time step for the subsonic algorithm was obtained for $\lambda = 2$, but again this had to be increased for the high h cases in order to avoid divergent behavior. All the results presented here have been obtained by imposing a limit of ten to the number of iterations in the second sweep. The total procedure converged (average error of the total displacement $\le 10^{-6}$) in about 50-80 time cycles for $h \le 2$ depending on the value of the stepsize Δx (for lower values of x more iterations were needed). A typical calculation required about 2-3 min of computer time (AMDAHL 470), a very small amount for a subsonic triple-deck solver. Convergence became very difficult for $h > 4$ and the same phenomenon observed in Ref. 11 for the highest Reynolds number case was encountered. The solution, while steadily converging everywhere else, presented an oscillatory behavior in time near the reattachment region, probably due to a "source effect" induced by the switching of the finite-difference representation (forward-backward) of the longitudinal convective term. Upwinding the normal convective term was found marginally helpful, and a way for completely eliminating such an oscillatory behavior around reattachment, was to set both convective terms equal to zero whenever the coefficient u^* (here taken as $(u_1^* + u_2^0)/2$) in the longitudinal convective term uu_x of the momentum equation was found to be negative. In this way, solutions were obtained for a smooth quartic hump for a reasonably large separation region.[24] Reducing the stepsize Δx in order to obtain a more accurate solution though inevitably led to divergent behavior. Such a phenomenon is exactly equivalent to what has already been encountered in high Re separated flow solutions of the interacting boundary-layer equations.[11] It is believed to be a numerical difficulty and not an indication of any hydrodynamic instability as has been claimed by some authors.

Acknowledgments

This research was supported by the Office of Naval Research under Contract ONR-N00014-76-C-0364, and the Naval Ship Research and Development Center under Contract N00014-76-C-0359.

References

[1] Brown, S. N. and Stewartson, K., "Laminar Separation," *Annual Review of Fluid Mechanics*, Vol. 1, 1969, pp. 45-72.

[2] Stewartson, K. and Williams, P. G., "Self-Induced Separation," *Proceedings of the Royal Society of London*, A 312, 1969, pp. 181-206.

[3] Stewartson, K., "Multistructured Boundary Layers on Flat Plates and Related Bodies," *Advances in Applied Mechanics*, Vol. 14, 1974, pp. 146-239.

[4] Sychev, V. Ya., "Concerning Laminar Separation," *Izvestiya Akademii Nauk Armyanskoi SSR, Mekhanika*, Zhidk Gaza No. 3, 1972, pp. 47-59.

[5] Neiland, V. Ya., "Towards a Theory of Separation of the Laminar Boundary Layer in a Supersonic Stream," *Izvestiya Akademii Nauk Armyanskoi SSR, Mekhanika,* Zhidk Gaza, No. 4, 1969.

[6] Neiland, V. Ya., "Flow Beyond the Separation Point on the Boundary Layer in Subsonic Stream," *Izvestiya Akademii Nauk Armyanskoi SSR, Mekhanika*, Zhidk Gaza, No. 3, 1971.

[7] Messiter, A. F., "Boundary Layer Flow Near the Trailing Edge of a Flat Plate," *S.I.A.M. Journal of Applied Mathematics*, Vol. 18, 1970, pp. 241-247.

[8] Smith, F. T., "Laminar Flow Over a Small Hump on a Flat Plate," *Journal of Fluid Mechanics*, Vol. 57, 1973, pp. 803-829.

[9] Stewartson, K., "On Laminar Boundary Layers Near Corners," *Quarterly Journal of Mechanics and Applied Mathematics*, Vol. 23, 1970, p. 137; "Corrections and Addition," Vol. 24, 1971, p. 387.

[10] Burggraf, O. R., Rizzetta, D., Werle, M. J., and Vatsa, V. N., "Effect of Reynolds Number on Laminar Separation of a Supersonic Stream," *AIAA Journal*, Vol. 17, April 1979, pp. 336-344.

[11] Napolitano, M., Werle, M. J., and Davis, R. T., "Numerical Solutions for High Reynolds Number Separated Flow," AIAA Paper 78-56, Huntsville, Ala., Jan. 1978.

[12] Williams, P. G., "A Reverse Flow Computation in the Theory of Self-Induced Separation," Proceedings of the 4th International Conference Numerical Methods in Fluid Dynamics, *Lecture Notes in Physics*, Vol. 35, Springer-Verlag, New York, 1975.

[13] Jenson, R., Burggraf, O., and Rizzetta, D., "Asymptotic Solution for Supersonic Viscous Flow Past a Compression Corner," Proceedings of the 4th International Conference on Numerical Methods in Fluid Dynamics, *Lecture Notes in Physics*, Vol. 35, Springer Verlag, New York, 1975.

[14] Rizzetta, D., "Asymptotic Solution for Two-Dimensional Viscous Supersonic and Hypersonic Flows Past Compression and Expansion Corners," Ph.D. Dissertation, The Ohio State University, 1976.

[15] Jenson, R., "Numerical Solution of Weakly Separated Flows at High Reynolds Number," Ph.D. Dissertation, The Ohio State University, 1977.

[16] Jobe, C. E. and Burggraf, O. R., "The Numerical Solution of the Asymptotic Equations of Trailing Edge Flow," *Proceedings of the Royal Society of London*, A 340, 1974, pp. 91-111.

[17] Chow, R. and Melnik, R. E., "Numerical Solutions of the Triple-Deck Equations for Laminar Trailing-Edge Stall," Proceedings of the 5th International Conference on Numerical Methods in Fluid Dynamics, *Lecture Notes in Physics*, Vol. 59, Springer Verlag, New York, 1976.

[18] Messiter, A. F. and Enlow, R. L., "Model for Laminar Boundary Layer Flow Near a Separation Point," *S.I.A.M. Journal*, Vol. 25, 1973, pp. 655.

[19] Smith, F. T., "The Laminar Separation of an Incompressible Fluid Streaming Past a Smooth Surface," *Proceedings of the Royal Society of London*, A 356, 1977, pp. 443-463.

[20] Werle, M. J. and Vatsa, V. N., "A New Method for Supersonic Boundary Layer Separation," *AIAA Journal*, Vol. 12, Nov. 1974, pp. 1491-1497.

[21] Rosenhead, L. (Ed.), *Laminar Boundary Layers*, Oxford University Press, Oxford, England, 1966.

[22] Blottner, F. G., "Computational Techniques for Boundary Layers," AGARD Lecture Series No. 73, Feb. 1975, pp. 3-9.

[23] Sykes, R. I., "Stratification Effects in Boundary Layer Flow Over Hills," submitted to *Proceedings of the Royal Society of London*.

[24] Napolitano, M., Werle, M. J., and Davis, R. T., "Numerical Soilutions of the Triple-Deck Equations for Supersonic and Subsonic Flow Past a Hump," University of Cincinnati, Dept. of Aerospace Engineering, AFL Rept. No. 78-6-42, 1978.

[25] Smith, F. T., private communication, Jan. 1978.

[26] Carnahan, B., Luther, H. A., and Wiles, J. O., *Applied Numerical Methods*, John Wiley & Sons, Inc., New York, 1969.